

Developments in Predicting Subcooled Flow Boiling CHF

Young Min Kwon^{*} Soo Dong Suk^{*}, and Soon Heung Chang^{**}

^{*} Korea Atomic Energy Research Institute

^{**} Korea Advanced Institute of Science and Technology

Abstract

A two-phase flow model was developed to predict a critical heat flux (CHF) in the subcooled and low quality flow boiling. The CHF formula was derived from the local conservation equations of mass, energy and momentum, together with appropriate constitutive relations. The limiting transverse interchange of mass flux crossing the interface of the bubbly layer and core region is represented, in the local momentum conservation equation, by taking account of the convective shear effects due to the drag force on the wall-attached bubbles. Comparison between the predictions by the proposed model and the experimental CHF data from several sources shows good agreement over a wide range of flow conditions ($2 \leq P \leq 20$ MPa, $1 \leq D \leq 37.5$ mm, $0.035 \leq L \leq 6$ m, $450 \leq G \leq 7500$ kg/m²s, $\alpha_{\text{exit}} \leq 0.8$). Also the model correctly accounts for the effects of flow variables.

1. Introduction

Critical heat flux (CHF) of subcooled flow boiling has received very much attention for the evaluation of upper limit of heat removal in boiling heat transfer system. For analysis and design purposes, reliable prediction methods are required. However, unfortunately the knowledge is not sufficient to predict the CHF with the desired degree of accuracy. The complication of a CHF problem for forced convection boiling is caused by the large number of variable factors and the variety of two-phase flows. In order to understand the physical nature of the CHF phenomenon, various mechanistic CHF models have been proposed so far.

Chang and Lee [1] presented a mechanistic model of CHF based on the bubble crowding mechanism, where the CHF formula was derived from mass, energy and momentum balance equations. In the present study, some significant modifications are made on the physical concept of a CHF mechanism and on the relevant constitutive relations in the earlier Chang and Lee's model. The proposed model is validated on the experimental CHF data of water in uniformly heated tubes and compared with the prediction using the CHF look-up table of Groeneveld et al. [2].

2. Phenomenological CHF Model

Most of the existing mechanistic models are based on the hypothetical flow structure or the limited experimental observation at CHF condition. A physical image of the boiling structure considered in this study is shown in Fig. 1, where the transverse interchange crossing the interface of the bubbly layer and core is shown. The flow is divided into two regions. In the outer annular layer of the round tube, attached bubbles are packed on the wall just prior to agglomeration and in the middle of the tube is a mixture core consisting of liquid and bubbles. The flow structure is based on the experimental observation by Gunther [3] and Kirby et al. [4] that the two-phase layer of local vapor film in subcooled flow boiling was an order of one bubble thickness. The present study uses the general approach of Weisman and Pei [5]. However, the effective thickness of bubbly layer is considered as a single bubble diameter, because it is assumed that only the wall-attached bubbles play the effective physical barrier to the heat transfer from the wall and the liquid supply from the core. Yagov et al.[6]

adopted a similar configuration of bubbly layer with a single bubble thickness for their semi-empirical CHF model under highly subcooled condition.

In the case of high subcooling and high mass flow rates, bubbles do not detach from their nucleation sites because bubbles are small enough to prevent bubble detachment from the wall by forces exerted by the bulk fluid. Furthermore the bubbles attached to the wall are condensed rapidly by highly subcooled core flow. However, bubble detachment is the normal case in the moderate subcooled flow boiling. As the wall reaches a required superheat temperature, the mean bubble diameter is sufficiently large to allow this bubble to detach from, or slide along, the wall. For both cases of the attached bubbles and detached bubbles, bubbles are assumed to be packed in a most dense array on the wall at near CHF condition.

Generally, active nucleation site density drastically increases when heat flux approaches to the CHF. As the number of bubbles surrounding one bubble becomes numerous, bubbles laterally coalesce on the wall and a bubbly layer may be made. It is assumed that CHF condition reaches at a certain void fraction in the bubbly layer (called critical void fraction) when radial thermal transport is limited by equal flows inward and outward at the interface of the bubbly layer and core. If the wall heat flux exceeds the maximum permissible heat flux satisfying the limiting condition above, the liquid in the bubbly layer depletes then dry spot area rapidly increases, and consequently the CHF occurs. The thermal transport limitation is governed by local mass, energy, and momentum balance equations based on the assumption that subcooled flow boiling CHF is a local phenomenon. The limiting transverse interchange of mass flux crossing the interface of the bubbly layer and core is determined by a momentum balance equation.

Beattie [7] has shown that the wall-attached bubbles act as a surface roughness equivalent to bubble size. Under such a condition, the friction factor can be described by the same form of equation as that used for a single-phase flow in roughened tubes. Although Beattie considered the flow remote from the CHF, it can be supposed that bubbles in the CHF region behave similarly. Also, for predicting the pressure drop in the subcooled flow boiling channel, Jia and Schrock [8], and Lu and Jia [9] proposed mechanistic models based on the enhanced friction coefficient due to the wall-attached bubbles. Their models could give a satisfactory agreement with experimental data. In the present work, the wall-attached bubbles are considered as increasing the roughness of the tube. The existence of roughness changes the hydrodynamic characteristics of the flow and the effect of viscous shear due to molecular friction becomes relatively small.

In the present study, one-dimensional steady state subcooled flow boiling in a tube is analyzed

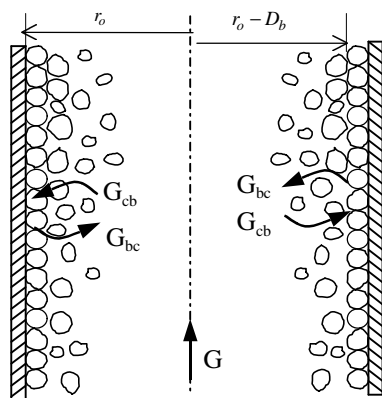


Fig. 1. Schematic diagram for the physical model

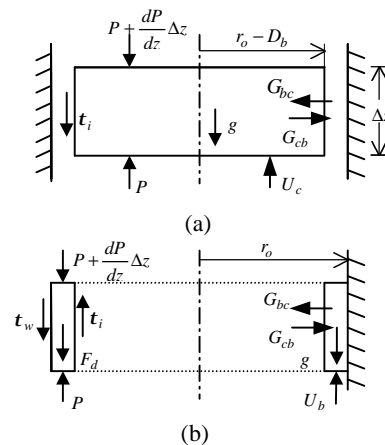


Fig. 2. Separated flow control volume for (a) core region and (b) bubbly layer

with the effects of two-phase flow models and constitutive equations. The basic assumptions of the present model for mathematical formulation are: (1) Two-phase flow structure at near CHF condition always takes the form of semi-reversal-annular flow pattern as shown in Fig. 1. (2) All the flow parameters except velocity are uniform across the tube cross-section. (3) The flows in the core and bubbly layer are each homogeneous. (4) The flow is steady. (5) The axial change of pressure is negligible compared with the system pressure. (6) The bubbly layer thickness is very small compared to the tube radius.

The governing equations are derived by applying the basic local conservation rules for mass, energy, and momentum to the control volumes such as that shown in Fig. 2(a) and 2(b). Considering the bubbly layer control volume of Fig. 2(b), total mass and energy balances, are given as below, respectively.

$$\frac{dG_b A_b}{dz} + G_{bc} \mathbf{x}_i - G_{cb} \mathbf{x}_i = 0 \quad (1)$$

$$\frac{dG_b A_b h_b}{dz} + G_{bc} h_b \mathbf{x}_i - G_{cb} h_c \mathbf{x}_i - q_w'' \mathbf{x}_w = 0 \quad (2)$$

G_{cb} and G_{bc} are the total inward and outward mass fluxes at the interface of the bubbly layer and core. ξ_i and ξ_w are the perimeters of the interface and the heated wall, respectively, i.e., $\xi_i = \pi(D - 2D_b)$ and $\xi_w = \pi D$, where D_b is the detached bubble diameter determined by the subcooled flow boiling model. Considering the relation of h_b in Eq. (11), two equations of (1) and (2) can be combined into Eq. (3). The variation of saturation properties of liquid and vapor in the axial flow direction is neglected because the pressure drop along the tube is small compared to the system pressure. Since the void fraction in the bubbly layer α_b is limited at the CHF condition, the quality in that layer has a finite value, i.e., $dx_v/dz = 0$, with the assumption of homogeneous flow.

$$q_w'' = G_{cb} (h_b - h_c) \frac{\mathbf{x}_i}{\mathbf{x}_w} \quad (3)$$

It is assumed that the wall-attached bubbles act as a surface roughness equivalent to bubble size. Chen [10], and Taylor and Hodge [11] reported that the flow resistance of a rough surface is divided into two components - that due to the form drag on the roughness element and that due to the viscous shear on the smooth surface area between the roughness elements. Based on the one-dimensional momentum equation of a separated flow model, momentum balances between shear forces, drag forces, and pressure on the control volumes of the bubbly layer and core are written, respectively, as.

$$-\frac{dP}{dz} + \frac{\mathbf{t}_i \mathbf{x}_i}{A_b} - \frac{\mathbf{b} \mathbf{t}_{w,v} \mathbf{x}_w}{A_b} - \frac{F_d N_{bub}}{A_b dz} - \mathbf{r}_b g + \frac{\mathcal{D}_{cb} \bar{U}_c - G_{bc} \bar{U}_b \dot{\mathbf{x}}_i}{A_b} = \frac{1}{A_b} \frac{d}{dz} \mathcal{E}_b \bar{U}_b^2 A_b \mathbf{j} \quad (4)$$

$$-\frac{dP}{dz} - \frac{\mathbf{t}_i \mathbf{x}_i}{A_c} - \mathbf{r}_c g + \frac{\mathcal{D}_{bc} \bar{U}_b - G_{cb} \bar{U}_c \dot{\mathbf{x}}_i}{A_c} = \frac{1}{A_c} \frac{d}{dz} \mathcal{E}_c \bar{U}_c^2 A_c \mathbf{j} \quad (5)$$

The number of attached bubbles along dz in the bubbly layer is, $N_{bub} = \pi D dz / D_b^2$, when bubbles are arranged in a rectangular lattice with a pitch of D_b . As in Taylor and Hodge, the apparent wall shear stress τ_w is defined as the sum of the viscous shear $\tau_{w,v}$ and form drag forces on the wall. The parameter F_d is the drag force which the rough element of a single bubble exerts on the flow field, and β ($0 < \beta < 1$) is the blockage factor that represents the area of the smooth surface between bubbles that is open for flow. As a first approximation, the drag force is assumed to be $F_d = \lambda \rho_c U_c^2 / 2 \times (\pi D_b^2 / 4)$, which is the same approach as done in Staub's [12] subcooled boiling model. The bubbly layer probably acts like a random roughness found in commercial tubes, because the bubbles are growing and collapsing on the heated wall. Therefore, the turbulent skin friction coefficient λ is calculated using the Colebrook-White equation with a two-phase Reynolds number ($Re_{2\phi} = GD / \mu_{2\phi}$) to account for the variation of the fluid viscosity near the heated wall.

Subtracting Eq. (4) from Eq. (5) to eliminate the pressure gradient term in the left-hand side, we obtain the limiting transverse interchange of mass flux at the interface of the bubbly layer and core

$$G^* = \frac{M}{(1-h_c)A} - \frac{t_i x_i}{(1-h_c)A} + \frac{b t_{w,v} x_w}{(1-h_c)A} - b_c - r_b g + \frac{p D F_d}{D_b^2 (1-h_c)A} + \Phi_{acc} \frac{h_c (1-h_c)}{(\bar{U}_c - \bar{U}_b) x_i} \quad (6)$$

with the definitions of the acceleration term.

$$\Phi = \frac{1}{A_b} \frac{d}{dz} \bar{e}_b \bar{U}^2 A_b - \frac{1}{c} \frac{d}{dz} \bar{e}_c^{-2} A_c j \quad (7)$$

The fraction of cross-section occupied by core is expressed by $\eta_c = A_c/A$. At CHF condition, the transverse mass transport rate at the interface is limited, i.e., $G^* = G_{bc} = G_{cb}$. The average fluid velocity of bubbly layer \bar{U}_b is determined by taking it as half the velocity of the core at the outer edge of bubbly layer, because the velocity profile in the bubbly layer is near linear. That assumption is valid for the case that the thickness of the bubbly layer is much smaller than the tube radius. Therefore, the variation of shear stress across the thin bubbly layer can be disregarded, i.e., $|\tau_i| \cong |\tau_{w,v}|$. The universal logarithmic velocity profile for a single-phase turbulent flow proposed by Von Karman is assumed to be valid in the turbulent core region.

If we assume that the bubbly layer behaves like the boundary layer region in a single-phase pipe flow, then the wall shear stress $\tau_{w,v}$ can be calculated from the Newton's viscous law using the universal velocity profiles. According to the rough calculation, i.e., $\tau_{w,v} = \mu_b (\partial u / \partial y) = \mu_b (2 \bar{U}_b / D_b)$, the effects of shear stresses are negligible compared to the other terms in the bracket of Eq. (6) for both cases of $\beta=0$ and 1. Also, Chang and Lee [1] have shown that the acceleration term Φ_{acc} is negligibly small with respect to the radial mixing flow effect. Therefore, for simplicity in this calculation, the first and second shear stress terms, and the acceleration term in the bracket of Eq. (6) are disregarded. This approach may seem crude, but the results are not strongly affected by the simplified assumption. Finally the CHF formula is expressed as a simple form from Eq. (3) and (6).

$$q''_{CHF} = \frac{M}{A_b} - r_c g + \frac{p D F_d}{D_b^2 (1-h_c)A} \frac{h_c (1-h_c)}{(\bar{U}_c - \bar{U}_b) x_w} \quad (8)$$

As shown in Eq. (8), accurate predictions of flow enthalpy and density at the location of the CHF occurrence are very important. In the case of uniform heating, the CHF usually occurs at the end of the heated tube. Assuming homogeneous flows of the bubbly layer and core, the quantities at the tube exit are defined as below.

$$\mathbf{a}_c = \frac{1}{h_c} \mathbf{a}_{avg} - \frac{1-h_c}{h_c} \mathbf{a}_b \quad \mathbf{m}_f = \mathbf{m}_f (1 - \mathbf{a}_{avg}) (1 + 2.5 \mathbf{a}_{avg}) + \mathbf{m}_g \mathbf{a}_{avg} \quad (9)$$

$$\mathbf{r}_b = \mathbf{r}_f (1 - \mathbf{a}_b) + \mathbf{r}_g \mathbf{a}_b \quad \mathbf{r}_c = \mathbf{r}_l (1 - \mathbf{a}_c) + \mathbf{r}_g \mathbf{a}_c \quad (10)$$

$$h_b = h_f (1 - x_b) + h_g x_b \quad h_c = h_l (1 - x_c) + h_g x_c$$

(11)

The average viscosity of core region μ_{20} is evaluated by Beattie and Whalley [13]. The average void fraction α_{avg} is determined by the subcooled flow boiling model.

In order to achieve closure of the mass, energy and momentum balance equations, several constitutive relations are required. For prediction of actual flow quality and enthalpy at the location of CHF occurrence, the void fraction profile in the subcooled flow boiling is determined by the Levy's model [14]. The flow quality was examined by both profile-fit and mechanistic approaches according to Lahey and Moody [15]. Because little difference in the CHF prediction appeared when both approaches were applied to the present CHF model, the simple profile-fit model of Saha and Zuber [16] is utilized. Once the flow quality at the tube exit is determined, the α_{avg} is calculated using the Zuber and Findlay [17] model, modified by Dix [18], which successfully covers a wide range of

pressure, flow, and void fraction.

The CHF formula of Eq. (8) is a function of fluid transport properties and geometry parameters. The drag force due to the wall-attached bubbles represents the characteristic parameter for radial turbulent interchange between the bubbly layer and core. It indicates that both hydrodynamic and thermal factors play a role in the onset of CHF in the present model.

3. Comparison with Experimental Data

To assess the predictive capabilities and the limitations of the proposed model, a total of 5009 water CHF data points, covering a wide range of different parameters, is obtained from the KAIST CHF database [19]. The range of parameters for each data source, considered in this study, is presented in Table 1, which covers the operating ranges of typical light water reactor (LWR) [20-24]. These data points, satisfying the condition that the void fraction at the tube exit is not greater than 0.8, are selected by using the subcooled flow boiling model and flow quality-void model before beginning the CHF calculation. Predictions using the present theoretical CHF model are compared with the experimental CHF data by examining the statistical results of CHF_R, defined as the predicted CHF to the measured CHF.

A best set of α_b , resulting in an average CHF_R of 1.0 while minimizing root-mean-square (RMS) error, were investigated by varying its value against the data points of Table 1. As a result, the correlation of Eq. (12) was obtained, which is shown by the curve in Fig.3.

$$\alpha_b = 0.83 - 0.29 e^{-4.71 x_{em} - 1.89} \quad (12)$$

Figure 4 shows the visual comparison of the predicted and measured CHF using the above data set. Most of the experiment data (about 93%) are successfully predicted within $\pm 20\%$ error band. The standard deviation σ and RMS error of CHF_R are 11.12% and 11.14%, respectively. If we restrict the application range of exit void fraction less than 0.7, about 97% of the total 3498 data is predicted within $\pm 20\%$, with μ (average value of CHF_R) = 1.02, σ = 8.91%, and RMS = 9.2%, while 99% data is predicted within $\pm 30\%$ error band.

The dependence of the prediction accuracy on major parameters is presented in Fig. 5 to Fig.7, where the CHF_R is plotted versus pressure, mass flux, and exit void fraction, respectively. A comparison of theoretical predictions from the present CHF model with experimental data does not seem to exhibit systematic deviations. However, the predictions at the low pressure region (less than 7 MPa) are generally underestimated as shown in Fig. 5.

For comparing with the present model, the predictions using the CHF look-up table of Groeneveld et al.[2] are performed based on the so-called heat balance method (HBM). The average value of the CHF_R is 1.02. The standard deviation and RMS error are 7.93% and 8.11%, respectively. Figure 8

Table 1. Experimental conditions for selected CHF data

Parameter	No.	D (m)	L (m)	P (MPa)	G (kg/m ² s)	Δh_{in} (kJ/kg)	x_{em}	q''_{CHF} (kW/m ²)
Thomson & Macbeth (1964)	1122	~ 0.038	~ 1.97	~ 18.96	~ 7499	~ 1659	~ 0.41	~ 14800
Becker et al. (1971)	804	~ 0.004	~ 4.97	~ 20.0	~ 7438	~ 1372	~ 0.60	~ 7480
Zenkevich (1974)	2925	~ 0.005	~ 6.0	~ 19.62	~ 6694	~ 1621	~ 0.62	~ 7290
Tong (1964)	123	~ 0.006	~ 3.66	~ 13.79	~ 7499	~ 1060	~ 0.38	~ 5900
Maylinger (1967)	35	0.007	~ 0.98	~ 10.24	~ 3734	~ 278	~ 0.21	~ 2860
Total	5009	~ 0.0011	~ 6.0	~ 20.0	~ 7499	~ 1659	~ 0.62	~ 14800

shows percentage of data points calculated with a given error band ($\pm\%$) for both the look-up table and the present model. As shown in Fig.8, the prediction accuracy of the look-up table is better than the present model for the entire range considered in this study. However, for subcooled conditions when the equilibrium quality at the tube exit is less than zero, the prediction accuracy of the present model is better than the CHF look-up table. About 96% of the total 902 data is predicted within $\pm 20\%$ error band, with $\mu = 0.995$, $\sigma = 8.75\%$, $RMS = 8.76\%$, respectively. While the Lookup table of Groeneveld et al. predicts 93% of the 899 data within $\pm 20\%$, with $\mu = 1.02\%$, $\sigma = 10.97\%$, $RMS = 11.12\%$, respectively.

Figure 9 shows that the parametric trends of CHF predicted by the present model are in good agreement with the data of Weatherhead [25]. The statistical analysis of the CHF values for 48 data points shows $\mu = 0.98$, $\sigma = 10.42\%$, $RMS = 10.57\%$, respectively, which are obtained without modification of Eq. (8). Also shown in Fig. 9 is the influence of inlet subcooling on CHF in the relatively high pressure region (13.8 MPa). The CHF increases almost linearly with inlet subcooling but its effect decreases with decreasing mass flux. The trends agree with general understanding regarding the CHF characteristics. The effect of liquid subcooling on CHF is prominent because the subcooled liquid flow condenses steam bubbles and suppresses their coalescence on the wall.

Figure 10 shows the effect of mass flux on CHF with the pressure as another independent variable, where CHF increases with increasing mass flux. The effect of mass flux depends on the system pressure such that it is stronger at lower pressure regions. The experimental data in Fig. 10 are directly taken from the CHF look-up table of Groeneveld et al. [2] for an 8 mm diameter tube based on reference exit quality, $x_{em} = -0.2$.

The effect of tube diameter on CHF is predicted by the present model, together with the interrelation between tube diameter and inlet subcooling $\Delta h_{sub,in}$ as shown in Fig. 11. The CHF increases with increasing tube diameter at fixed inlet conditions. The effect increases with the increase of the inlet liquid subcooling. For tubes of diameter other than 8 mm, the diameter correction factor suggested by the table authors was used. For small tube diameters, the prediction by the present model agrees well with the CHF look-up table, however, the difference between two predictions increases as the tube diameter increases.

It is a general understanding that CHF is a decreasing function of tube length for fixed inlet conditions. The present model follows well the general trends of experimental data as shown in Fig. 12. It is noted that data points shown in the figure are only for the cases where the 1995 CHF look-up table data are available with a heat balance equation. The CHF decreases more rapidly for short tubes and the length effect seem to disappear for longer tubes.

4. Conclusion

As a conclusion, an advanced mechanistic CHF model using two-phase flow model has been developed to predict the CHF during the subcooled and low quality flow boiling in a uniformly heated vertical tube. Comparison of the current model predictions to the experimental CHF data shows a good agreement over a wide range of LWR operating conditions. It can be suggested that the dominant mechanism controlling the CHF in the subcooled and low quality flow boiling is properly represented in the present model. It is suggested that refinement of this model should be pursued in the future to improve the critical void fraction in the bubbly layer. Furthermore, an improvement in the current model can readily be made if better constitutive laws are used for the complex boiling phenomena.

Acknowledgements : This work was performed under the Long-term Nuclear R&D Program sponsored by the Ministry of Science and Technology.

Nomenclature

A	cross-section area,	x_{em}	equilibrium quality,	bc	bubbly layer to core,
D	tube diameter,	α	void fraction,	c	core,
D_b	bubble diameter,	ρ	density,	cb	core to bubbly layer,
G	mass flux,	μ	viscosity,	f	saturated liquid,
g	gravity acceleration	σ	surface tension,	g	vapor phase,
h	enthalpy,	τ	shear stress,	i	interface
P	pressure,	ζ	perimeter,	l	subcooled liquid,
q''	heat flux,	<u>subscripts</u>		w	heated wall.
U	mean velocity,	b	bubbly layer,		
x	flow quality,				

References

- S. H. Chang and K. W. Lee, Nucl. Eng. Des., 113, 35-50 (1989).
- D. C. Groeneveld, L. K. H. Leung, P. L. Kirillov, et al, Nucl. Eng. Des., 163, 1-23, (1996).
- F. C. Gunther, TRANS. ASME, 73, 115-121 (1951).
- G. J. Kirby, R. Stainiforth, and L. H. Kinneir, AEEW-R-506, UKAEA (1967).
- J. Weisman and B. S. Pei, Int. J. Heat Mass Transfer, 26, 1463-1477, (1983).
- V. V. Yagov and V. A. Puzin, Thermal Engineering 32, 569 (1985).
- D. R. H. Beattie, NUREG/CP-0014, p.1343 (1980).
- D. Jia and V. E. Schrock, 4th Miami Int. Symp. On Multi-phase Transport and Particular Phenomenon, (1986).
- S. Lu and D. Jia, Experimental Heat Transfer, Fluid Mechanics, and Thermodynamics, Edited by R. X. Shah, R. N. Ganic, and K. T. Yang, Elsevier Science Publishing Co. Inc. (1988).
- C. K. Chen, Ph.D thesis, Washington State University (1971).
- R. P. Taylor and B. K. Hodge, ANL/ESD/TM-31, Argonne National Laboratory (1992).
- F. W. Staub, J. Heat Transfer 90, 151-157 (1968).
- D. R. Beattie and P. B. Whalley, Int. J. Multiphase Flow, 8, 83-87 (1982).
- S. Levy, Int. J. Heat Mass Transfer, 10, 951 (1967).
- R. T. Lahey, Jr. and F. J. Moody, The Thermal-Hydraulics of A Boiling Water Nuclear Reactor, ANS, Second ed., La Grange Park, Illinois (1993).
- P. Saha and N. Zuber, Proc. 5th Int. Heat Transfer Conf., Tokyo, Japan, Vol. 4, p.175 (1974).
- N. Zuber and J. Findlay, J. Heat Transfer, 87, 453-462, (1965).
- G. E. Dix, NEDO-10491, General Electric Company (1971).
- S. H. Chang, W. P. Baek, and S. K. Moon, KAIST-NUSCOL-9601 (1996).
- B. Thompson and R. V. Macbeth, AEEW-R-356 (1964).
- K. M. Becker and G. Strand, KTH-NEL-14 (1971).
- A. Zenkevich, AECL-Tr-Misc-304 (1974)
- F. Maylinger, EUR-3347, (1967).
- L. S. Tong, Westinghouse report WCAP-3736, (1964).
- R. J. Weatherhead, ANL-6675, (1963), cited from J. G. Collier and J. R. Thome, Convective Boiling And Condensation, Clarendon Press, 3rd edn. Sect. 8.2, (1994).

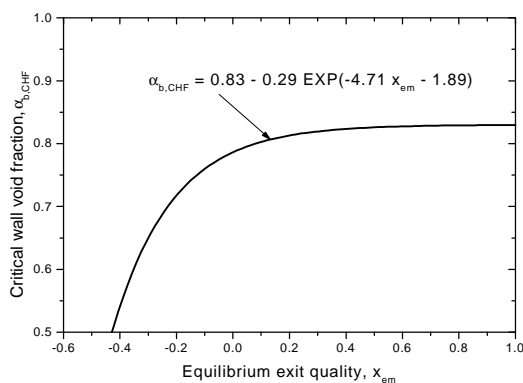


Fig. 3. Correlation of critical void fraction in the bubbly layer.

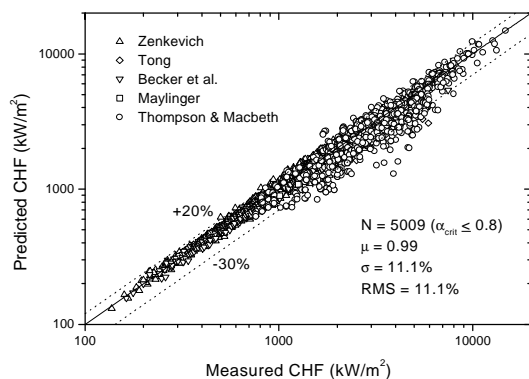


Fig. 4. Predicted vs experimental CHF.

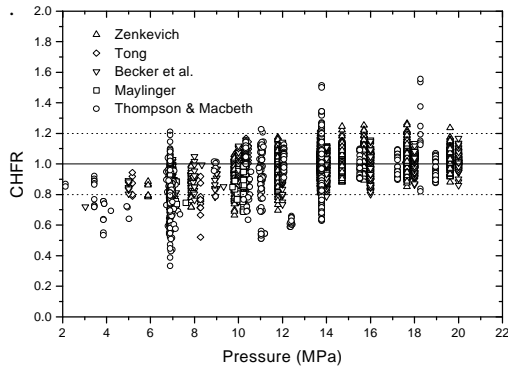


Fig. 5. CHF vs pressure

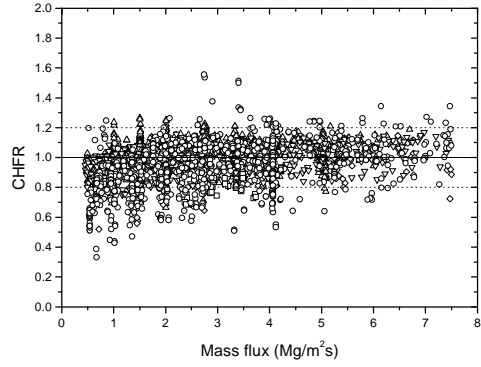


Fig. 6. CHF vs mass flux.

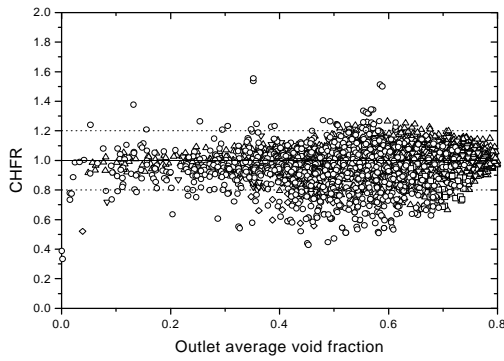


Fig. 7. CHF vs average void fraction

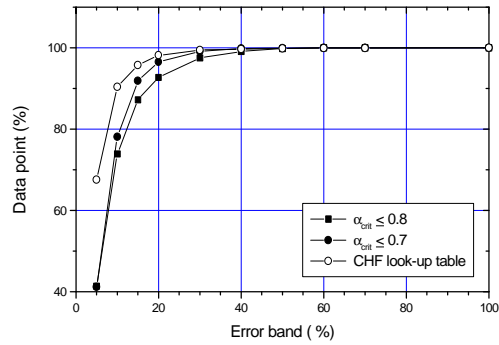


Fig. 8. Percentage of data points predicted within error band

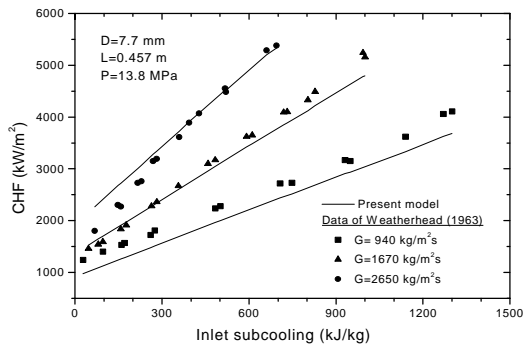


Fig. 9. Comparison of predicted CHF with Experimental data of Weatherhead (1963)

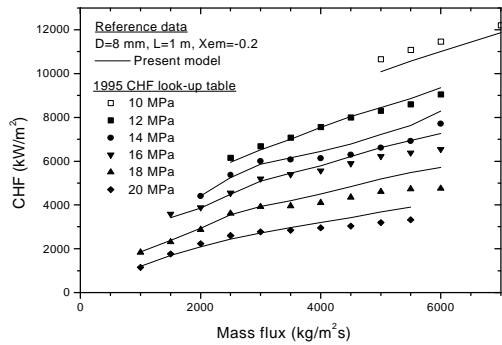


Fig. 10. Prediction of mass flux effect on CHF

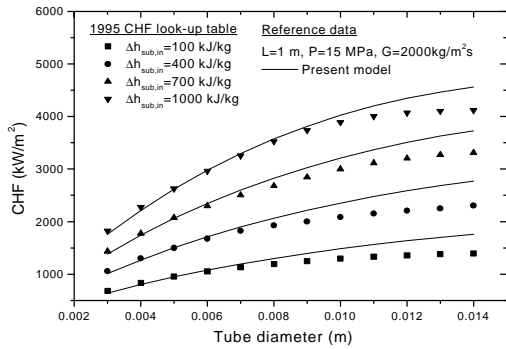


Fig. 11. Prediction of tube diameter effect on CHF

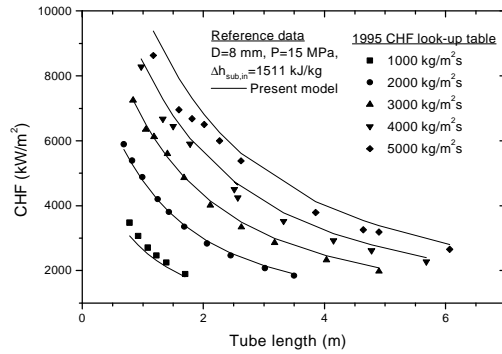


Fig. 12. Prediction of heated length effect on CHF